Effect of High Temperature on Bond Strength of FRP Rebars

By Ammon Katz,[1] Neta Berman,[2] and Lawrence C. Bank,[3] Member, ASCE

Abstract: The bond properties of fiber reinforced polymer (FRP) reinforcing bars (rebars) at temperatures ranging from room temperature (20°C) to high temperatures of up to 250°C are discussed in this paper. The bond properties in this temperature range were studied for a number of commercially produced rebars, where different bond "treatments" were applied to FRP rebars. Test results showed a reduction of between 80 and 90% in the bond strength as the temperature increased from 20 to 250°C. In comparison, ordinary deformed steel rebars showed a reduction of only 38% in the same temperature range. In addition, a reduction in the bond stiffness, which was determined from the slope of the ascending branch of the pullout load versus slip curve, was seen as the temperature increased. At elevated temperatures the postpeak bond decrease was gradual as compared with the instantaneous drop at room temperature. Greater sensitivity to high temperatures was seen in FRP rebars, in which the bond relies mainly on the polymer treatment at the surface of the rod.

INTRODUCTION

Fiber reinforced polymer (FRP) rebars are being used increasingly in construction where ordinary steel reinforcement is not suitable due to highly corrosive environments or where electromagnetic transparency of the structure is required. High temperatures, such as those due to fires or even those occurring in extremely hot climates, may decrease the properties of these rebars. The mechanical properties (especially the strength and the stiffness) of polymers are known to decrease significantly as the temperature is increased and the polymer approaches its glass transition temperature T_g (Fried 1995). Thermosetting polymers (e.g., vinyl ester and polyester) are currently being used as the matrix materials in FRP rebars. It is well known that these polymers have glass transition temperatures in the range of 60–130°C, with the higher transition temperatures for the vinyl ester resins. It is therefore to be expected that the mechanical properties of the rebars themselves will be affected as the temperature approaches and passes through the glass transition temperature of the polymer resin.

High-performance inorganic and organic fibers, such as glass, carbon, and aramid fibers, are being used in FRP rebars (Yamasaki et al. 1993). These fibers exhibit good mechanical property retention in the elevated temperature range considered in this work (up to 250°C) (Dostal 1987), and it is expected that failure of the rebars at high temperature will occur first in the polymer matrix. High-temperature tests of the properties of a variety of FRP rebars were conducted by Kumahara et al. (1993), who found a reduction of ~20% in the tensile strength of glass and carbon FRP rebars at a temperature of 250°C. The reduction of tensile strength of aramid FRP rebars was greater and was ~60% at 250°C. The effect of matrix composition appeared to be relatively small. Fujisaki et al. (1993) reported a reduction of 40% in the tensile strength of glass-carbon FRP grids at a temperature of 100°C, probably due to changes in the properties of the polymer that forms the grid; however, no further reduction was seen for higher temperatures of up to 250°C. The impact resistance of concrete members (curtain walls) reinforced with the FRP grids at high temperature was good, and Fujisaki et al. (1993) concluded that these concrete members would perform satisfactorily in the event of a fire. Wolff and Miesseler (1993) proposed giving prestressed concrete members reinforced with glass FRP tendons the same consideration for fire protection as that given for steel tendons, due to the small reduction in the tensile strength of glass FRP tendons, which was similar to that seen for steel tendons.

On the other hand, Wang and Evans (1995) reported a reduction of 75% in the flexural strength of FRP beams as the temperature was increased from room temperature to 300°C. Partially prestressed concrete beams were tested by Okamoto et al. (1993) to investigate their performance in a fire. The prestressing tendons were made of aramid FRP, and the reinforcement was made of either aramid or carbon FRP rebars. Failure of the beams occurred when the temperature of the reinforcement reached ~200°C and ~300°C for the aramid and carbon rods, respectively. The failure occurred at relatively low temperatures despite the good high-temperature tensile characteristics of the rods themselves and the small initial stress applied before heating (~15% of the tensile strength).

The discrepancies in these results are explained by the differences in the properties of FRP composites in different orientations, which is due to the anisotropy of the composite material. In the direction of the fibers (i.e., the longitudinal or axial direction of the rebar), the properties are governed by the properties of the fibers, which exhibit good performance at high temperature. The polymer largely governs the properties in the transverse direction, such as shear in a plane parallel to the fiber direction. Therefore a reduction in the shear strength of an FRP rebar is expected as the temperature increases. This reduction explains the aforementioned results of Wang and Evans (1995), as the flexural strength of a composite beam relies on the transfer of shear stress through the polymer.

It is expected that in reinforcing applications the longitudinal strength of FRP rods will not be significantly affected in a temperature range of up to 300°C. However, the bond strength of FRP rebars to the surrounding concrete is primarily a function of the properties of the polymer at the surface of the rod (Bank et al. 1998), mainly, its shear strength. Therefore, it is expected that when dealing with the effect of temperature on FRP reinforced concrete, the bond strength of FRP rebars will be affected first as the temperature increases.

[1]Sr. Lect., Nat. Build. Res. Inst., Dept. of Civ. Engrg., Technion-Israel Inst. of Technol., Haifa 32000, Israel. E-mail: akatz@techunix.technion.ac.il

[2]Grad. Student, Nat. Build. Res. Inst., Dept. of Civ. Engrg., Technion-Israel Inst. of Technol., Haifa 32000, Israel.

[3]Prof., Dept. of Civ. and Envir. Engrg., Univ. of Wisconsin, Madison, WI 53706. E-mail: bank@engr.wisc.edu

Note. Discussion open until October 1, 1999. To extend the closing date one month, a written request must be filed with the ASCE Manager of Journals. The manuscript for this paper was submitted for review and possible publication on July 14, 1998. This paper is part of the ***Journal of Composites for Construction***, Vol. 3, No. 2, May, 1999. ©ASCE, ISSN 1090-0268/99/0002-0073–0081/$8.00 + $.50 per page. Paper No. 18790.

EXPERIMENTAL PROGRAM

Materials

Rods

Four types of FRP rebars were tested and compared with ordinary deformed steel rebars. The four types of FRP rebars are shown in Fig. 1. The nominal diameter of the FRP rebars was 12.7 mm (#4), and the diameter of the ST rebar was 12.0 mm. The actual diameter of the FRP rebars was somewhat larger, depending on the surface treatment of each one. Properties of the FRP rebars are given in Table 1.

Different surface treatments were applied to the FRP rebars to enhance the bond to concrete as can be seen in Fig. 1. Large deformations were molded on the polymer at the surface of the CB rebars, giving these bars lugs with a similar geometry as those found on ordinary steel deformed reinforcing bars. A helical braid of glass fibers was wound on the CPH, CPI, and NG rebars. The braid was narrow for the CPH and NG rebars and wide for CPI rebar (Fig. 1); in addition, the braid was wrapped tightly around the NG rebar, which produced large convex protrusions on the surface of the rebar.

Embedded sand particles on the surface of the CPH and NG rebars was used as an additional means to enhance the bond for these rebars. The sand was dispersed evenly on the surface of the CPH rebars in a very thin layer of polymer, which was similar to the polymer in the core of the rebar. The external layer of polymer used in the NG rebar was different from the one in the core; it was relatively thick (1–2 mm) and partially obscured the deformations created by the tight wrapping of the helical strand that was wrapped on the core fibers. The sand was embedded unevenly on the surface of this rebar.

Roughening the surface of the CPI rods were achieved by leaving excess polymer resin on the surface of the rebar during production. This excess polymer resin hardened after polymerization and formed irregularities (small bumps and "blobs") on the surface of the rebars.

Concrete

Normal strength concrete with a 28-day compressive strength of 35 MPa was used. The composition of the concrete was as follows: ordinary portland cement, 348 kg/m^3; water, 195 kg/m^3; coarse aggregate, 1,059 kg/m^3; and sand, 733 kg/m^3. Superplasticizer in the amount of 0.85% by weight of cement was used. Concrete slump was 5 in. which allowed for good compaction around the rods without excess bleeding.

The effect of high temperature on the compressive strength of the concrete was tested on 100- × 100- × 100-mm concrete cubes. At the age of 28 days the cubes were placed in an oven at temperatures of 10, 220, and 330°C for 90 min and tested immediately after being removed from the oven.

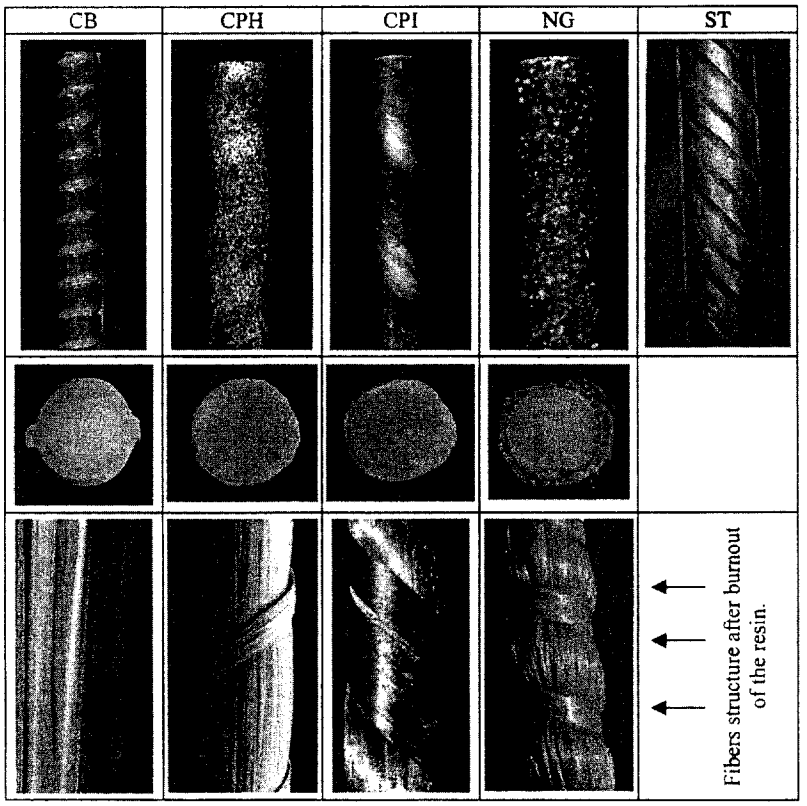

FIG. 1. Images of Tested FRP Rebars

TABLE 1. Properties of FRP Rebars Tested

Rod type (1)	Nominal diameter (mm) (2)	Type of resin in core (3)	Physical bond improvement to surface of rebar (4)	Space between deformations/windings (mm) (5)	Glass transition temperature (°C) (6)
CB	12.7	Urethane modified vinyl ester	Large deformations	7.5	124
CPH	12.7	Epoxy vinyl ester	Helix + sand coating	27	122
CPI	12.7	Epoxy vinyl ester	Helix + resin roughening	25	95
NG	12.7	Polyester (assumed)	Helix + sand coating + deformations	12	60
ST	12.0	Steel	Large deformations	7.7	—

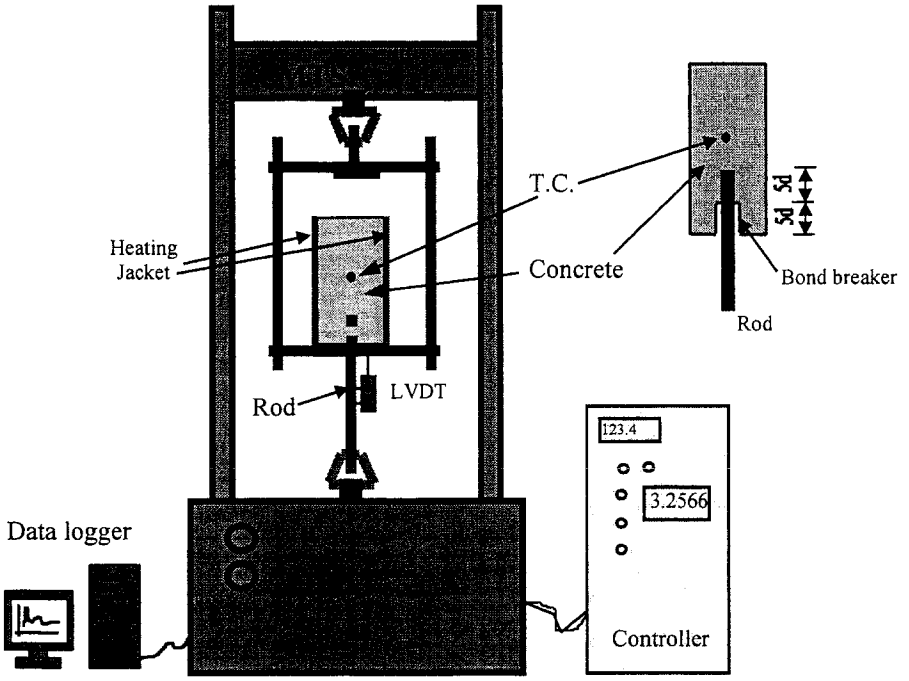

FIG. 2. Test Setup

Test Setup

Cylinders with a diameter of 150 mm and a length of 300 mm were prepared. The rebars were placed vertically in the bottom of the molds before casting. The embedment length was 60 mm (5 diameters). A bond breaker with a length of 60 mm (5 diameters) was inserted around the rebar at the concrete surface, in accordance with RILEM/CEB/FIB recommendations ("Bond" 1977). A thermocouple (TC) was placed at the center of the mold near the rebar surface, before casting, to measure the internal temperature at the rebar surface during the tests (Fig. 2).

Specimens were demolded after 1 day and stored in water at 20°C until the age of 7 days. They were then moved to standard laboratory conditions (21°C, 60% relative humidity) and cured until the age of 28 days or more (up to 90 days). An early study showed no difference in the bond strength between 28 and 90 days of age.

A special heating jacket was fabricated to heat the specimens. The jacket wrapped the specimen and allowed the specimen to be heated at a high heating rate of ~5°C/min. This heating rate is close to the rate of temperature rise during a fire. The close contact of the heating jacket with the specimen allowed the specimen to be heated without the need for special heat resistance loading or measuring equipment. The setup is shown in Fig. 2.

Two types of experiments were performed as follows:

- STRL—heating the specimen up to the desired temperature and then performing a pullout test at a constant slip rate
- SLRT—loading the specimen to a prescribed load and then heating the specimen until pullout began

A typical plot showing the temperature rise at the center and at the surface of the concrete cylinder is shown in Fig. 3. The temperature rise at the center of the cylinder was initially at a rate of 5°C/min; however, at ~120°C a temporary plateau in the temperature rise was seen. At that temperature a significant escape of vapor from the specimen was observed. The vapor escaped from the outer surface of the concrete cylinder and from the area around the bond breaker at the rebar location.

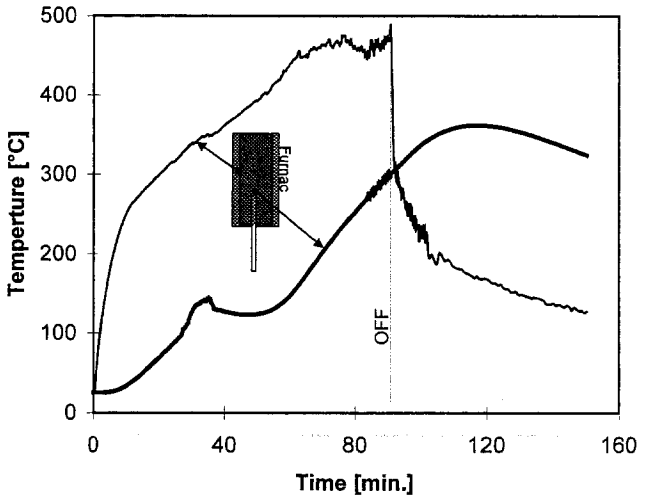

FIG. 3. Typical Diagram of Temperature Rise in Specimen

After completion of the evaporation the temperature continued to rise at the same rate as the initial rate.

From Fig. 3 it can be seen that turning the heating jacket off did not immediately stop the temperature rise at the center of the concrete cylinder due to the thermal inertia of the massive concrete cylinder. The temperature continued to rise for an additional 50–60 degrees following shutoff of the heat. Therefore, in the STRL experiments, the heating jacket was shut off when the temperature was ~10°C less than the specified testing temperature, and pullout was performed a few minutes after this when the rate of heating decreased. A temperature rise of ~20°C was recorded during the whole test. The temperature shown in the results is the temperature reading at the time when peak load was reached.

A typical diagram of pullout test in the SLRT test procedure is shown in Fig. 4. The specimen was loaded up to a prescribed load at room temperature; then the heating was started and continued until a sudden slip occurred. The temperature at which the rebar began to slip was considered to be the failure temperature.

Nominal bond strength τ was calculated using (1), which

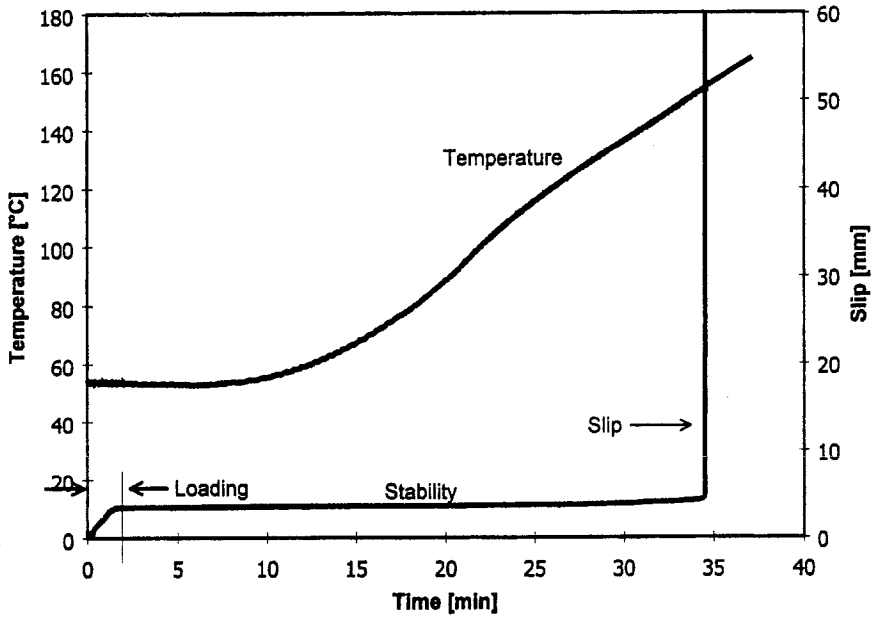

FIG. 4. Typical Diagram of Pullout in SLRT Setup

assumes uniform distribution of the bond stress along the embedment length l

$$\tau = \frac{P_{max}}{\pi d l} \tag{1}$$

where d = rebar nominal diameter; l = embedment length; and P_{max} = peak load during pullout. Since the rebars all had the same nominal diameter and bond length, comparison between them can also be made based on the pullout load rather than the bond strength.

Results

Bond Strength

The effect of temperature on the bond strength calculated by (1) is shown in Fig. 5 for CB, CPH, CPI, NG, and ST rebars. Results from both test setups are shown in Fig. 5.

Similar trends can be seen for all of the FRP rebars; relatively high bond strength is seen at room temperature, with the exception of NG rebar, which had a polymer of poor properties in the external layer. The bond strengths at room temperature of CB, CPH, and CPI rebars were 13.2, 12.2, and 10.9 MPa, respectively. These values are similar or somewhat larger than the bond strength of the ST rebar (11.2 MPa). At temperatures in the range of 80–160°C a reduction in the bond strength was seen for all of the FRP rebars. At ~200°C the bond strength leveled off and remained almost constant as the temperature was increased, as can be seen in Fig. 5. Experiments were stopped at around 300°C. At higher temperatures (400°C and above) the polymer matrix will begin to decompose (Prian et al. 1997; Gentry et al. 1998); no mechanical properties can be expected at these temperatures. Values of bond strength at room temperature, the residual bond at high temperature, and the degree of bond strength reduction are listed in Table 2.

NG rebar was the most sensitive to temperature rise and lost its bond strength rapidly at relatively low temperature. Loss of 55% of the bond strength was seen at a temperature of 92°C, though the entire loss of bond was "only" 80% compared with the other FRP rebars (85–92%). Rapid reduction in bond strength was also seen for CB rebars in which most of the reduction was in the 80–150°C range. The reduction in bond strength of the CPH and CPI rebars occurred over a wider range and extended up to 200°C.

Reduction in the bond strength as temperature increased was also seen in the ST rebars (Fig. 5). At 200°C the bond loss was ~40%, compared with bond loss of >80% for the FRP rebars. An additional increase in the temperature produced a very moderate additional loss of bond strength and the values remained relatively high. These findings are in good agreement with the findings of Diederichs and Schneidwe (1977).

When the specimens were tested in the SLRT mode, failure of the bond was seen at ~120°C regardless of the type of rebar or the preloading level. At failure, extensive exhausting of water vapor (steam) at the interface between the rebar and the surrounding concrete was seen. It appears that the flux of vapor outward at high pressure stimulated the slippage of the rebars, leading to premature failure at that temperature. When the specimens were slowly dried in an oven at 100°C prior to the test, this phenomenon was avoided, and the results obtained were similar to the results in the STRL mode. The results shown in Figs. 4 and 5 for the SLRT mode represent the tests of the predried specimens.

Reduction in the bond strength can be partially attributed, in some cases, to the reduction in the strength of the concrete seen in Fig. 6. A reduction of ~15% was seen at a temperature of 200°C, with some increase thereafter. These findings are typical of the behavior of concrete at high temperature as described by Malhotra (1982). Therefore, a reduction in the concrete strength can explain some of the reduction in bond strength at high temperature in the cases where the bond mechanism is mainly via the concrete, as discussed in the following.

For the ST rebars, the failure of the bond was by shear of the concrete surrounding the rod, between the deformations. Residues of the concrete could be seen between the deformations, after pullout, at all temperatures. For the FRP rebars at room temperature, some concrete residue could be seen adhering to the CPH and CPI rebars together with locations of abraded polymer at the surface of the rebars. Detailed discussion on the modes of failure at room temperature can be found in Katz (unpublished paper, 1998). At higher temperatures (above the T_g of the polymer at the rebar surface), no concrete residue was seen on any of the FRP rebars. On the contrary, residue of the polymer from the surface of the rebar was seen in the concrete after pullout, indicating an accelerated reduction in the properties of the polymer relative to the concrete. Therefore, it can be concluded that in the case of FRP rebars, the reduction in the bond strength at high temperature cannot

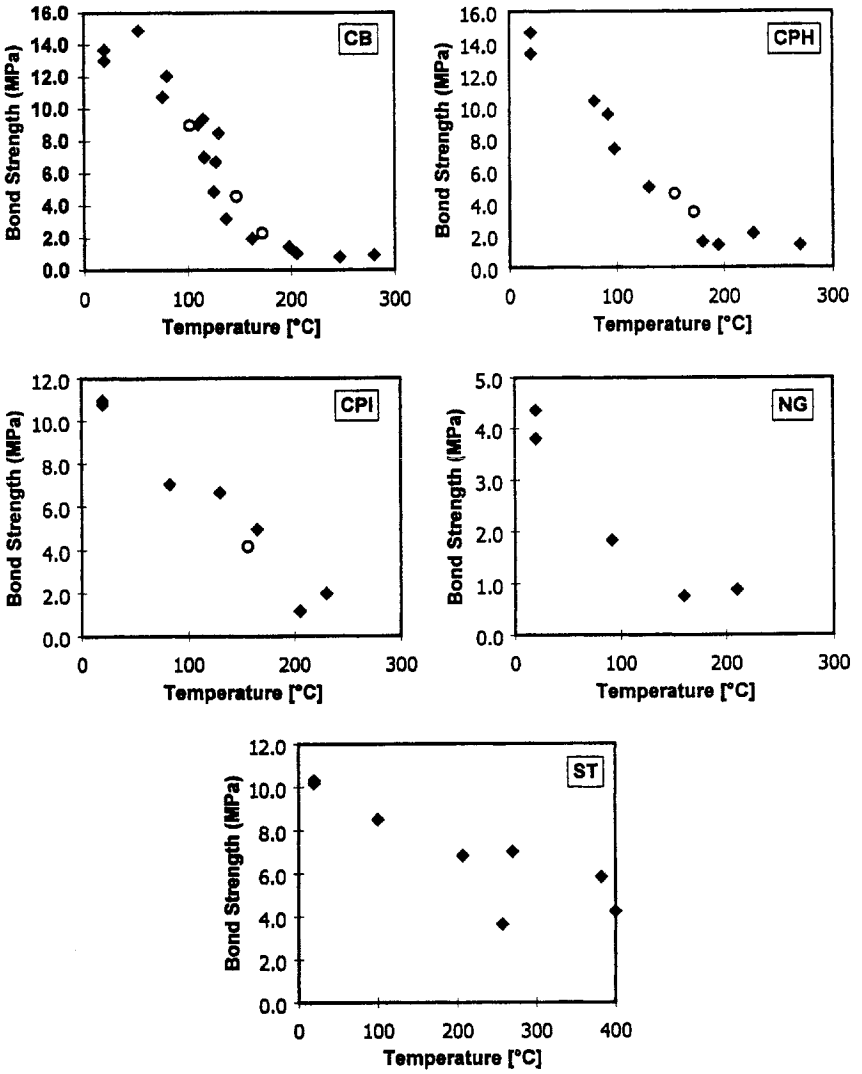

FIG. 5. Effect of Temperature on Bond Strength of Tested FRP Rebars (♦, STRL; ○, SLRT).

TABLE 2. Bond Strength Values at Room Temperature, Residual Bond Strength at Temperature above 200°C, and Amount of Bond Strength Loss

Rod type (1)	Bond Strength (MPa)		Loss of bond (%) (4)
	Room temperature (2)	Residual bond (3)	
CB	13.2	1.1	91.7
CPH	12.2	1.7	86.1
CPI	10.9	1.6	85.3
NG	4.1	0.8	80.5
ST	11.2	6.9	38.4

be attributed to the minor reduction in the strength of the concrete.

It appears that the presence of inorganic components (i.e., sand particles and helical fiber) on the surface of the FRP rebars contributes to the resistance to temperature rise. The effect of the elevated temperature was more critical for the rebars where the bond relies on the properties of the polymer, such as the CB (polymeric deformations) and NG (thick layer of polymer) rebars, than for the CPH and CPI rebars where the helical wrap of glass fibers was used. The effect of the sand particles is not clear as performance was similar for the CPI rebars where no sand was used at the surface and for the CPH rebars that had sand particles at the surface.

Complete Pullout Load versus Slip (P-s) Curve

P-s curves of the tested rebars at different temperatures are presented in Fig. 7. Two aspects are considered in the analysis of the complete *P-s* curves: (1) The changes in the prepeak; and (2) the changes in the postpeak part of the curves due to the rise in temperature.

Prepeak Behavior. The slope of the prepeak curve can be considered to be the "bond modulus" (or bond stiffness) because it gives a relationship between load and deformation. This value has an important effect on the width of primary flexural cracks in reinforced concrete and on the deflection of beams and slabs. The behavior of reinforced concrete members having rebars with different bond moduli may, therefore, be different despite similarities in bond strengths of the rebars. A reduction in the slope of the ascending curve was seen for almost all of the rebars tested, as the temperature increased. The results are presented in Fig. 8. The reduction appears to be linear for all of the FRP rebars; however, the mechanisms affecting this reduction are complicated, and the apparent linear behavior is probably a result of a combination of these different mechanisms.

Most theoretical models that describe the bond of reinforcing bars to concrete consider the rebar as a homogeneous material, which is much stiffer than the surrounding concrete. This assumption is appropriate for ordinary steel reinforcement. However, in the case of FRP rebars, the reinforcing bar, and primarily its surface layer at the concrete interface, is

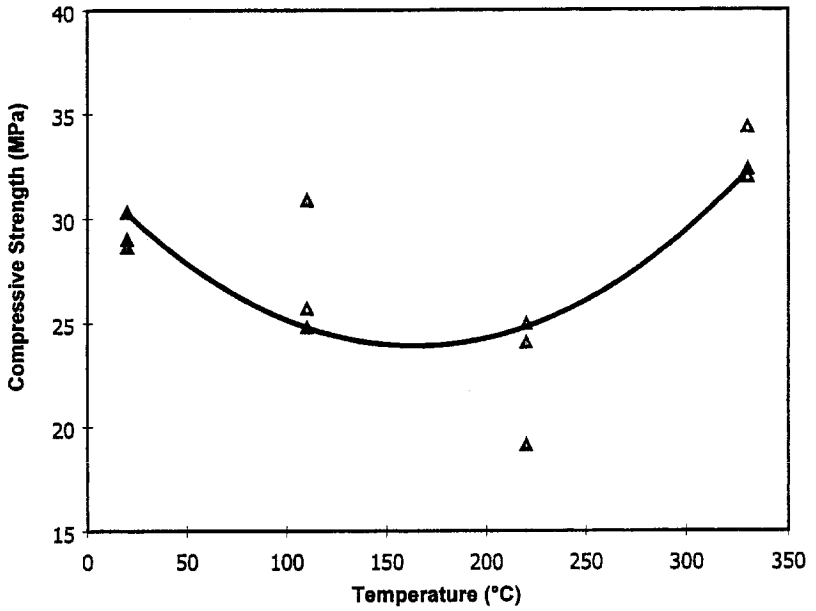

FIG. 6. Effect of Temperature on Compressive Strength of Concrete

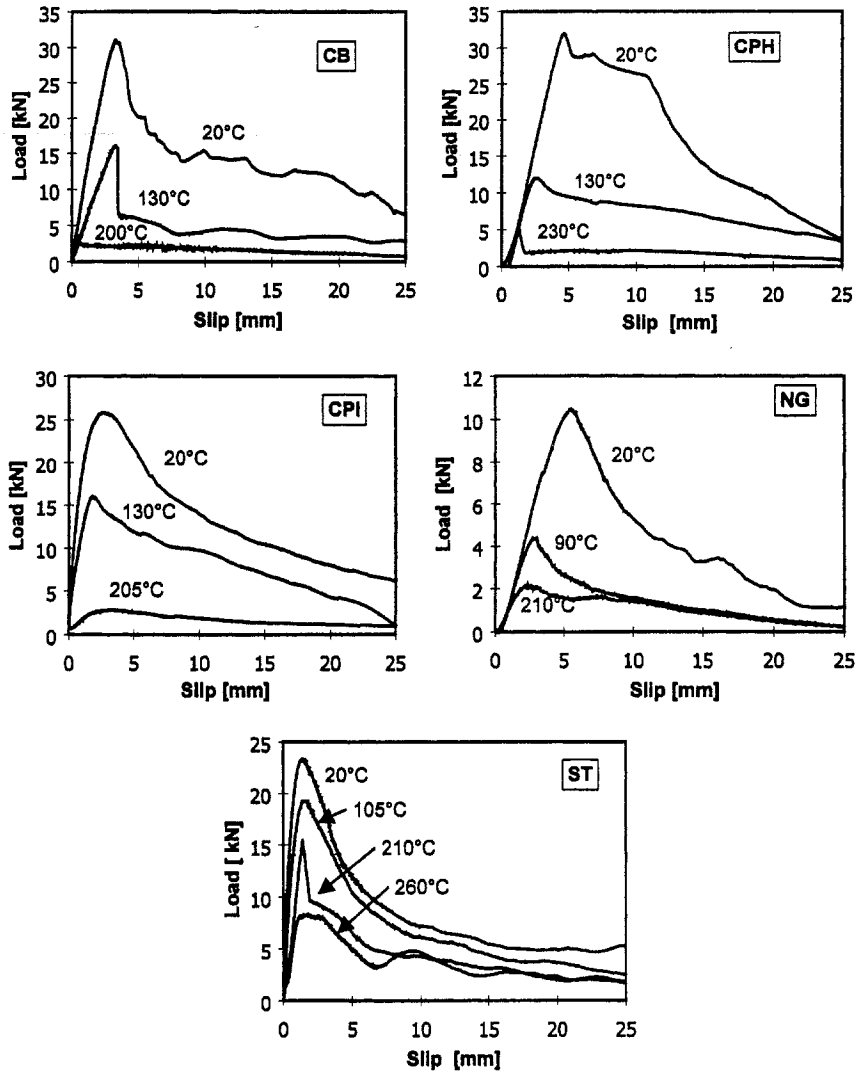

FIG. 7. Complete *P-s* Curves of Tested FRP Rebars at Different Temperatures

weaker and more flexible than the concrete, especially when the temperature increases.

The effect of temperature on the *P-s* relationships in the elastic zone can be described by the model presented by Greszczuk (1969) that was developed for the pullout of a rod (fiber in his case) that is perfectly bonded to a surrounding matrix. The slip is related to the quotient G_i/b, where G_i is the shear modulus of the external layer of the rod and the inter-

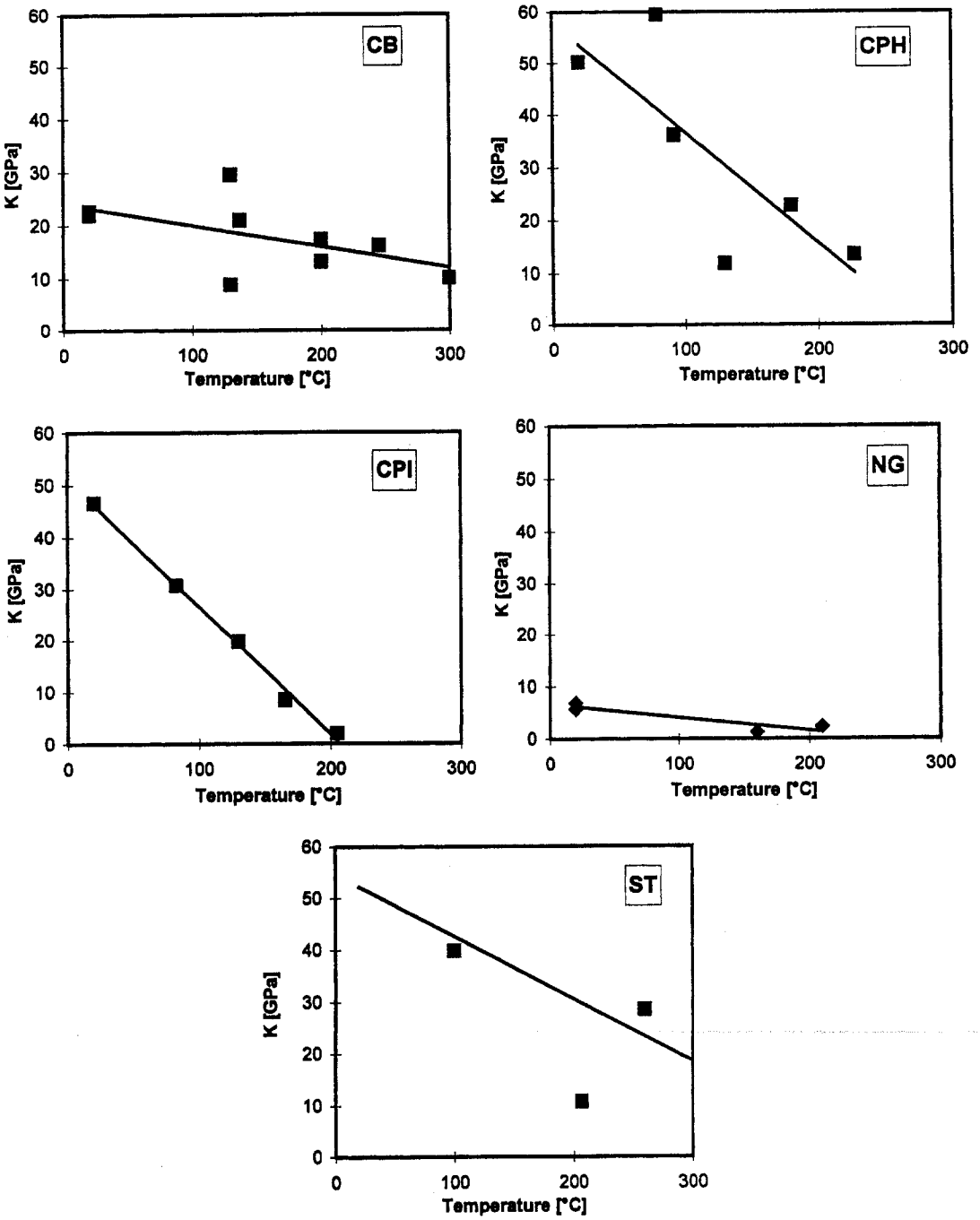

FIG. 8. Bond Modulus of Tested FRP Rebars

facial zone in the matrix (concrete) close to the rod, and b is its thickness. Other parameters, such as the longitudinal modulus of elasticity and the rod's radius are not significantly affected by the change in temperature in the range considered in this study. The key result obtained using Greszczuk's model is given in Appendix I. From the model it can be seen that increasing the temperature reduces the shear modulus of the external layer of the rod and also increases the thickness of this layer, due to the temperature gradient into the rod. These two mechanisms affect the bond modulus and lead to its reduction as the temperature increases. However, the relative contribution of each of these two mechanisms is not precisely known.

Postpeak Behavior. The postpeak behavior at room temperature can be divided into two stages: (1) Rapid reduction in the load bearing for a short distance after the peak; and (2) more moderate reduction thereafter (Fig. 7). The differences between the various surface treatments affect the rate of reduction in the load in Stage 1 and the final values of the load and slip in Stage 2. For the CB rebars, a steep reduction of 30–40% is seen immediately following the peak load. The load decreases gradually thereafter to a total slip of ~40 mm. At ~130°C a steep postpeak reduction is still seen; however, a constant low slip resistance (bond stress) is maintained following the drop. At a higher temperature of 200°C, a small peak is seen with a gradual decrease thereafter. The prepeak bond mechanism of these rebars relies on wedging of the lugs (deformations) in the surrounding concrete, whereas the postpeak bond is achieved through wedging of the broken lugs into the surface of the rod (Katz, unpublished paper, 1998). As the temperature increases, the surface layer with the lugs softens and becomes more flexible and weak, thus preventing the mechanism of wedging from being effective both in the prepeak and postpeak stages. Therefore, a rapid reduction in

the loads was seen after the peak, followed by a small load bearing after the reduction.

For the CPH rebars, the peak load is maintained for a slip of ~5 mm at room temperature. This is followed by a moderate reduction thereafter (Fig. 7). The total slip at which all bond was lost was ~30–35 mm. When the temperature increased, a moderate reduction was seen immediately after the peak to a complete reduction of the load, following a slip of ~35 mm. A similar trend was seen for CPI and NG rebars; however, at room temperature the peak load was not maintained as was seen for the CPH rods. As the temperature increases, the slope of the postpeak curve becomes more linear, and the sudden drop immediately after the peak disappears.

It appears that the differences between the postpeak behavior of these rebars, when compared with the CB rebars, is a result of the helical wrapping on the rods and to some extent the sand particles embedded on the surface. The bond mechanism in these rebars does not rely only on the polymer in the surface layer but also on additional features (i.e., the helical wrap and the sand particles), which are less sensitive to the effect of temperature. Thus the postpeak reduction is more moderate and exhibits constant bond strength to complete pullout (expressed by the linear reduction in the pullout load).

In the range of temperatures that the FRP rebars were tested, no significant change in the *P-s* behavior of the ST rods was seen. Generally, after the peak load was reached, a rapid decrease of about 50% of the load was seen, followed by a gradual decrease to complete pullout. This pattern was the same at all temperatures up to 210°C, though at decreasing levels of loads. As the bond mechanism of this type of rebar relies on mechanical anchoring to the concrete at all temperatures, no significant change is expected by the effect of temperature, except for a moderate general reduction resulting from the reduction in the concrete strength as discussed previously.

Images of Rebars' Surface after Pullout

Gradual yellowing of the surface could be seen for all of the FRP rebars as the testing temperature increased (Fig. 9). In addition, progressive damage to the surface of the rebars was seen, in the form of peeling of the external layer, ripping of the helix, and extensive abrasion as discussed in the following for each type of rebar.

Shearing of the lugs and increased yellowing was seen for CB rebars at temperatures up to 150°C. As the temperature further increased, the color became dark and extensive abrasion was seen in addition to the shearing of the lugs. Residues of glass fibers could be found in the concrete after pullout at a temperature of 250°C, indicating that the damage occurred at the core of the rod and was not only limited to the surface, as was seen at the lower temperatures.

No significant damage could be seen for CPH or CPI rebars when pulled at room temperature; the polymeric layer at the surface was slightly abraded, and some concrete residues had adhered to the surface, indicating a mixed damage of rod and the surrounding concrete (Fig. 9). When the temperature at pullout increased to 100°C, shearing of the external layer was observed. The external layer was completely stripped from the core, exposing the longitudinal fibers and the helix. However, no significant damage to the core was seen. With further increase of the temperature, up to 200°C, signs of damage to the core were seen; the helix separated from the core and broke, and signs of abrasion were seen on the naked core. Increasing amounts of polymer were found in the concrete after pullout, as the testing temperature increased, indicating that the external layer was removed from the surface and was not forced into the core during pullout. A unique phenomenon was seen for the NG rebars. At room temperature the outer layer of the rod was completely removed during pullout, exposing the

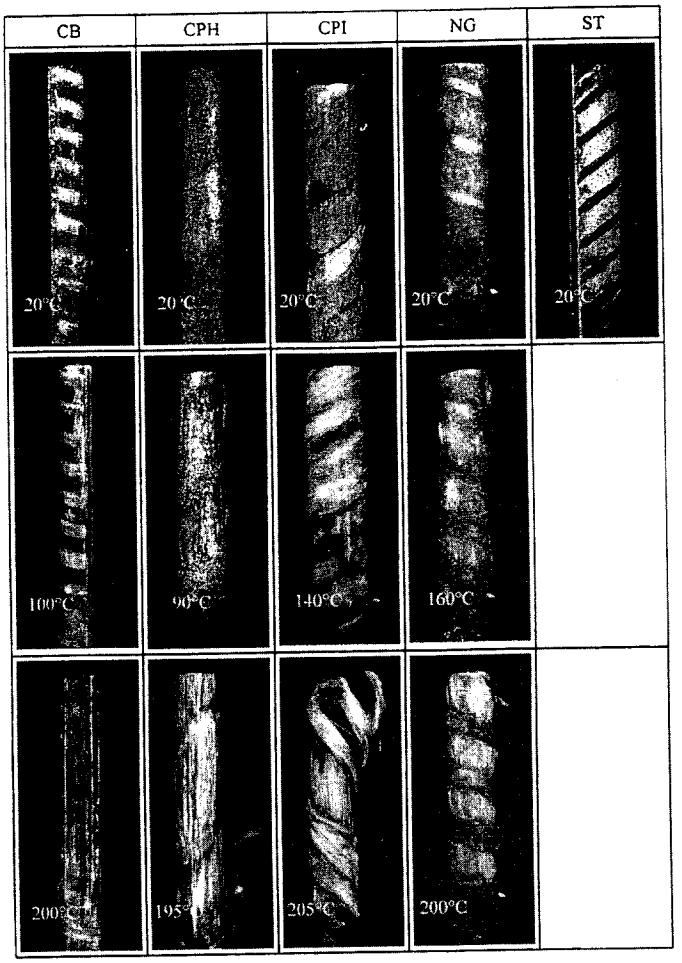

FIG. 9. Images of FRP Rebars after Pullout at Different Temperatures

core. As the temperature increased, the external layer was removed only from the convex parts of the core, between the windings of the helix. Residues of this layer were seen in the concave parts (on the rebar) over the windings. It appears that as the temperature increases, progressive reduction in the mechanical properties of the external layer takes place. Thus, internal shearing of this layer leaves residues of polymer in the concave regions. At high temperature, the damage became more extensive, leading, again, to a complete removal of this layer, as can be seen in Fig. 9.

Residues of concrete were found between the deformations of the steel bars for all the tested temperatures; thus only one picture was chosen for Fig. 9. It could be clearly seen that in all cases the failure of bond for these rebars resulted from failure of the concrete and not from failure of the rebars, as was seen in the FRP rebars.

DISCUSSION

It appears that the extent to which the bond mechanisms of an FRP rebar depend on the polymer at the rebar surface is the main parameter that influences the degradation in bond strength of FRP rebars to concrete at high temperatures. The bond properties of two types of rebars considered in this study (CB and NG) were found to rely solely on the polymer. In the former, large stiff lugs at the surface provide the bond strength at room temperature, whereas in the latter, a thick weak polymeric layer at the surface hides the deformations of the core and does not sufficiently support the sand particles embedded on the surface, which were presumably provided to enhance the bond. In both cases these rebars experience a rapid reduction in the bond strength as the temperature increases. The

differences between these two rebars can be seen in their postpeak behavior. Because some support is given to the external layer of the NG rebars by the helical wrapping, the reduction in load after the peak is relatively moderate, as compared with the steep postpeak reduction in the CB rebars, where the bond relies solely on the polymeric lugs.

Bonding systems that rely on wrapping of helical glass fiber with a thin layer of polymer at the surface of the rebar showed a better behavior, as was seen for rebars CPH and CPI. The reduction in bond strength as the temperature increased was more moderate, and the postpeak behavior was one of a gradual reduction in the load bearing rather than a sudden drop, as was seen in the case of the CB rebars. It is possible that the above changes could be a result of different properties of the polymers, mainly at the surface; however, a reduction in the mechanical properties of polymers is known to occur at their glass transition temperature T_g. Therefore, the reduction in bond, as seen in the rebars where the bond mechanisms relies only or mainly on the polymer, is quite expected.

The reduction in the bond strength could be attributed to loss of concrete strength at elevated temperature due to internal vapor pressure, which is the explanation for some reduction in the concrete strength and consequently to the loss of bond strength for ST rebars. However, because residues of polymer from the surface of the FRP rebars were found in the cavity in the concrete after complete pullout, it can be concluded that the reduction in bond strength can be attributed to the polymer in the surface of the rebar only. In addition, controlled drying of the specimens prior to testing in the second test setup (SLRT) revealed the same bond results, indicating that the reduction in the concrete properties was not the cause for the loss of bond strength at high temperature.

SUMMARY AND CONCLUSIONS

Different types of FRP rebars were tested for pullout at temperatures of up to 250°C. High values of bond strength were obtained at room temperature (in the range of 11–13 MPa) in all FRP rebars, except for one type of rebar that had a weak external layer where bond strength was only 4 MPa. The bond strength was as high or somewhat higher than the bond strength obtained for steel rebars (11 MPa).

The results showed a severe reduction in the bond strength as the temperature was raised to 180–200°C. A reduction of 92% was seen for CB rebars where the bond strength dropped from 13.2 to 1.1 MPa at a temperature of 250°C. The bond in this type of rebar is achieved through polymeric lugs (deformations), which appear to be more affected by the high temperature than other rebars. In CPH and CPI rebars, having helical wrapping of glass fiber around the core, the reduction in bond strength was smaller (from 12.2 to 1.7 MPa and from 10.9 to 1.6 MPa, respectively), though small bond values were obtained at high temperature for all of the FRP rebars. The bond strength reduction in the deformed ST rebars, in comparison, was from 11.2 to 6.9 MPa, in the same temperature range.

A thick polymeric layer at the surface as seen in NG rebars appears to negatively affect the bond both at room temperature and at 200°C (4.0 and 0.8 MPa, respectively).

Temperature also affects the bond modulus (the slope of the ascending P-s curve), which tends to decrease as the temperature increases. The descending curve of the FRP rebars becomes more linear as the temperature increases, indicating a degradation in the polymeric surface treatments that support the bond, leaving the rebar with only a friction mechanism to create a bond.

Extensive damage to the surface of the rod was seen as the temperature at which pullout of the rebar occurred rose, indicated by yellowing of the rebar and significant abrasion of the external layer.

APPENDIX I. GRESZCZUK'S (1969) MODEL FOR PULLOUT

Greszczuk's model is based on shear lag theory and assumes an interfacial transition zone between the rod (fiber) and the surrounding matrix. The shear stress along the rod $\tau(x)$ is determined according to the following:

$$\tau(x) = \frac{P\beta}{2\pi rr} [\sinh(\beta x) - \coth(\beta l)\cosh(\beta x)] \quad (2a)$$

$$\beta = \left(\frac{2G_i}{b_i rE}\right)^{0.5} \quad (2b)$$

where r = radius of the rod; b_i = effective width of the interface; E = longitudinal modulus of elasticity of the rod; G_i = shear modulus of the interface; l = embedded length; and P = pullout load.

APPENDIX II. REFERENCES

Bank, L. C., Puterman, M., and Katz, A. (1998). "The effect of material degradation on bond properties of FRP reinforcing bars in concrete." *ACI Mat. J.*, 95(3), 232–243.

"Bond test reinforcing steel—2. Pull-out test." (1978). RILEM/CEB/FIP Recommendation RC6 RILEM/CEB/FIP, Paris.

Diederichs, U., and Schneidwe, U. (1977). "Untersuchung des Verbundverhaltens und der Verbund-Festigkeit von Rippenstraben und Glatten Rundstaber bei Hohen Temperaturen." Institute Fur Baustoffkundeund Stahlbetonbau, Braunschweig, Germany (in German).

Dostal, C. A., ed. (1987). *Engineering materials handbook, Vol. 1: Composites*. ASM International, Materials Park, Ohio.

Fried, J. R. (1995). *Polymer science and technology*. Prentice-Hall, Englewood Cliffs, N.J., 167–169.

Fujisaki, T., Nakatsuji, T., and Sugita, M. (1993). "Research and development of grid shaped FRP reinforcement." *Proc., Fiber-Reinforced-Plastic Reinforcement for Concrete Struct.*, A. Nanni and C. W. Dolan, eds., American Concrete Institute, Detroit, 177–192.

Gentry, T. R., Bank, L. C., Barkatt, A., and Prian, L. (1998). "Accelerated test methods to determine the long-term behavior of composite highway structures subject to environmental loading." *ASTM J. of Composites Technol. and Res.*, 20(1), 38–50.

Greszczuk, L. B. (1969). "Theoretical studies on the mechanics of the fiber-matrix interface in composites." *Interfaces in Composites*, ASTM STP 452, ASTM, West Conshohocken, Pa., 42–58.

Kumahara, S., Masuda, Y., and Tanano, Y. (1993). "Tensile strength of continuous fiber bar under high temperature." *Proc., Fiber-Reinforced-Plastic Reinforcement for Concrete Struct.*, A. Nanni and C. W. Dolan, eds., American Concrete Institute, Detroit, 731–742.

Malhotra, L. (1982). *Design of fire-resistance structures*. Surrey University Press, London, 48–77.

Okamoto, T., Matsubara, S., Tanigaki, M., and Hasuo, K. (1993). "Practical application and performance of PPC beams reinforced with braided FRP bars." *Proc., Fiber-Reinforced-Plastic Reinforcement for Concrete Struct.*, A. Nanni and C. W. Dolan, eds., American Concrete Institute, Detroit, 875–894.

Prian, L., et al. (1997). "Use of thermogravimetric analysis to develop accelerated test methods to investigate long-term environmental effects on polymer composites." *High temperature and environmental effects on polymeric composites*, T. S. Gates and A. Zureick, eds., Vol. 2, ASTM STP 1302, ASTM, West Conshohocken, Pa., 206–222.

Wang, N., and Evans, J. T. (1995). "Collapse of continuous fiber composite beam at elevated temperatures." *Composites*, 26(1), 56–61.

Wolff, R., and Miesseler, H. J. (1993). "Glass fiber prestressing system." *Alternative materials for the reinforcement and prestressing of concrete*, J. L. Clarke, ed., Chapman & Hall, London, 34–54, 131–132.

Yamaski, Y., Masuda, Y., Tanano, H., and Shimizu, A. (1993). "Fundamental properties of continuous fiber bars." *Proc., Fiber Reinforced Plastic Reinforcement for Concrete Struct.*, A. Nanni and C. W. Dolan, eds., American Concrete Institute, Detroit, 715–730.